

3. PALEOCEANOGRAPHY OFF SANRIKU, NORTHEAST JAPAN, BASED ON DIATOM FLORA¹

Itaru Koizumi² and Tatsuhiko Sakamoto³

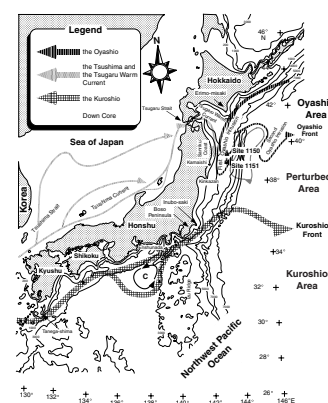
ABSTRACT

The diatom flora from two sediment cores recovered from the upper 27 meters below seafloor (mbsf) in the oceanic frontal area off Sanriku, northeast Japan, during Ocean Drilling Program Leg 186 were analyzed. Diatom abundance seems to be in interglacial stages and suggests a south-north shifting of the frontal area. Diatom temperature values are less reliable because frequency of the warm-water species is smaller. Site 1151 was in a warm climate at ~50 ka, as were Deep Sea Drilling Project Sites 579 and 580 in the western North Pacific Ocean. A mixed diatom assemblage in the upper 3 mbsf at Site 1150 is evidence that the Tsugaru Warm Current flowed into the studied area through the Tsugaru Strait.

INTRODUCTION

The sea off Sanriku, northeast Japan, north of ~38°N, is a thermal frontal area between the Oyashio Front and the Kuroshio Front (Fig. F1). Flowing along the coast of Japan and reaching ~35°N, the Kuroshio Current turns east and mixes with the cold, low-salinity Oyashio Current coming down from the Bering and Okhotsk Seas. At the northern margin of the frontal area, Oyashio water intrudes southward along the Sanriku Coast. The Tsugaru Warm Current, flowing from the Japan Sea into the Pacific Ocean through the Tsugaru Strait, flows southward, closer to the Sanriku Coast, and occasionally comes in contact with the

F1. Location of Sites 1150 and 1151, p. 10.



¹Koizumi, I., and Sakamoto, T., 2003. Paleoclimatology off Sanriku, northeast Japan, based on diatom flora. In Suyehiro, K., Sacks, I.S., Acton, G.D., and Oda, M. (Eds.), *Proc. ODP, Sci. Results*, 186, 1–21 [Online]. Available from World Wide Web: <http://www-odp.tamu.edu/publications/186_SR/VOLUME/CHAPTERS/110.PDF>. [Cited YYYY-MM-DD]

²Atsubetsu Kita 3, 5-18-2, Atsubetsu-ku, Sapporo 004-0073, Japan. itaru@sci.hokudai.ac.jp

³Institute for Frontier Research on Earth Evolution (iFREE), Japan Marine Science and Technology Center, Natsushima-cho 2-15, Yokosuka 237-0061, Japan.

Initial receipt: 2 January 2002

Acceptance: 3 October 2002

Web publication: 24 April 2003

Ms 186SR-110

Oyashio Intrusion, which elongates, forming a tongue-like shape ~160 km in width (Kawai, 1972).

The sea off northeast Japan is a crucial area for determining the hydrographic relationship between the equatorial Pacific and subarctic North Pacific Ocean over time. However, the northwest Pacific almost entirely lacks carbonate pelagic sediments containing foraminifers and coccolithophorids because its seafloor lies at depths largely below the calcium carbonate compensation depth. Diatom paleoceanographic analyses of the late Neogene on a north-south track across the subarctic front were unravelled during Deep Sea Drilling Project (DSDP) Leg 86 (Koizumi, 1985).

The high-resolution paleoceanographic analyses, however, off the coast of northeast Japan have not been performed because the hydraulic piston corer was not used in previous ocean drilling during DSDP Legs 56, 57, and 87 in the forearc area. Ocean Drilling Program (ODP) Leg 186 provided one opportunity for establishing a high-resolution profile of paleoceanographic history during the Quaternary off northeast Japan based on diatom flora.

MATERIALS AND METHODS

Site 1150 (39°11'N, 143°20'E; water depth = 2681 m) is located in the deep-sea terrace on the landward side of the Japan Trench. The upper 200 meters below seafloor (mbsf) of sediment from Hole 1150A consists of interbedded diatomaceous ooze and clay (Sacks, Suyehiro, Acton, et al., 2000). [Maruyama and Shiono](#) (this volume) suggest the sedimentation rate of 170.1 m/m.y. for the upper 51 mbsf, based on the last occurrence at 0.30 Ma of *Proboscia curvirostris* at 51.03 mbsf. The upper 27 mbsf of Hole 1150A was estimated to be late Quaternary in age and was utilized for this study (Table T1).

Site 1151 (38°45'N, 143°20'E; water depth = 2178 m) is located 48 km south of Site 1150, in the deep-sea terrace of the Japan Trench. The upper 100 mbsf of Hole 1151C is diatomaceous silty clay. The sedimentation rate is 38.3 m/m.y. based on the last occurrence of *P. curvirostris* at 11.50 meters composite depth (mcd). The upper 22 mbsf covers the latest Quaternary used in this study (Table T2).

Dried sample (0.10 g) was placed into a 100-mL beaker with ~10 mL of hydrogen peroxide solution (15%) for several seconds and then left to stand for 24 hr after diluting with distilled water. After pouring off the suspension, the residue was diluted again with 75 mL of distilled water and homogenized for ~3 s in an ultrasonic washer (Clean Matic; 20 W, 40 kHz). Using a micropipette (Justor-Jv 500 µL), 0.25 mL of the solution was placed on a cover glass (18 mm × 18 mm), dried on a hot plate at 50°C, and then mounted on a glass slide using Pleurax.

All diatoms were identified and counted until the number of individual specimens reached 200, excluding *Bacteriastrum* spp. and *Chaetoceros* spp. But only *Chaetoceros furcelatus* was counted.

Sediment accumulation rates were calculated on the basis of the diatom events.

APPROACH

Paleoceanographic analyses are undertaken on the basis of (1) diatom abundance (number of diatoms), (2) diatom temperature (*T_d*) val-

T1. Distribution chart of diatom species, Hole 1150A, p. 15.

T2. Distribution chart of diatom species, Hole 1151C, p. 16.

ues, (3) species composition, which reflects the effects of salinity of the water and mode of living, (4) number of extinct diatoms, and (5) principal component analysis, which uses the results from the previous four analytical methods for determining the composition of species.

Diatom Abundance

The number of diatom valves in a given volume of sediment depends on (1) diatom productivity, (2) preservation and/or dissolution of the diatoms, and (3) dilution with terrigenous and/or other organic materials.

Warm-Water and Cold-Water Diatoms

The warm-water (Xw) and cold-water (Xc) species have been classified according to Kanaya and Koizumi (1966). All these diatoms are living species.

Xw species are as follows:

Alveus marinus (Grunow) Kaczmarek and Fryxell
Azpeitia nodulifera (Schmidt) Fryxell and Sims
Coscinodiscus perforatus Ehrenberg
Fragilariopsis doliolus (Wallich) Medlin and Sims
Hemidiscus cuneiformis Wallich
Planktoniella sol (Wallich) Schtt
Rhizosolenia bergonii Peragallo
Roperia tessellata (Roper) Grunow
Thalassiosira leptopus (Grunow) Hasle and Fryxell

Xc species are as follows:

Actinocyclus curvatulus Janisch
Actinocyclus ochotensis Jouse
Asteromphalus robustus Castracane
Bacteriosira fragilis (Gran) Gran
Chaetoceros furcellatus Bailey
Coscinodiscus marginatus Ehrenberg
Coscinodiscus oculus-iridis Ehrenberg
Fragilariopsis cylindrus (Grunow) Krieger
Neodenticula seminae (Simonsen and Kanaya) Akiba and Yanagisawa
Odontella aurita (Lyngbye) Agardh
Porosira glacialis (Grunow) Jorgensen
Rhizosolenia hebetata forma *hiemalis* (Bailey) Gran
Thalassiosira gravida Cleve
Thalassiosira hyalina (Grunow) Gran
Thalassiosira nordenskiöldii Cleve
Thalassiosira trifulta Fryxell

Diatom Temperature Values

The Td ratio was proposed by Kanaya and Koizumi (1966) to estimate sea-surface water temperature during the accumulation of sediments in the lower levels of a core sequence:

$$Td = [Xw/(Xw + Xc)] \times 100,$$

where Xw is the frequency of warm-water diatoms and Xc is that of cold-water diatoms. Td ranges in value from 0 to 100. Going from the subarctic region to the tropical region, Td becomes systematically

larger, showing a positive correlation with sea-surface water temperature over a given geographical site in the North Pacific (Kanaya and Koizumi, 1966).

Species Composition

Diatom populations incorporated into the sediment of Sites 1150 and 1151 at the time of deposition include sublittoral diatoms (brackish water and meroplanktonic or tythropelagic species) and/or freshwater diatoms that are inferred to have been transported to the site by drainage from the land and downslope transport.

Extinct Diatoms

The core sediments include extinct diatoms that are present as a result of reworking Miocene to Pliocene sedimentary rocks on the sea-floor and/or inland area. The age of these rocks are identified according to diatom biostratigraphy.

Principal Component Analysis

Principal component analysis of diatom species was carried out when more than six valves of a given species were found in a sample in order to statistically analyze the stratigraphic assemblage structure which reflects the effects of physiographical-ecological, phytogeographical, and evolutionary factors at the site.

RESULTS OF PALEOCEANOGRAPHIC ANALYSIS

Hole 1150A

Diatom Abundance

The number of diatom valves varies from $1.6 \times 10^7/g$, the minimum value at 8.00 mbsf, to $18.4 \times 10^7/g$, the maximum at 1.85 mbsf (average = $7.2 \times 10^7/g$) (Fig. F2). Large fluctuations occur, with secondary and smaller fluctuations. The high values are observed at ~1.50, 17.00, and 26.20 mbsf. The large decreases occur at ~7.50 and 20.20 mbsf.

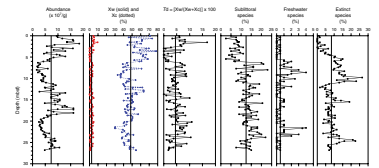
Warm-Water and Cold-Water Diatoms

Warm-water diatoms are overwhelmed by cold-water diatoms throughout the section. In the upper part, warm-water *Fragilariopsis dolius* and *Thalassiosira leptopus* are slightly more abundant and show the maximum of 9.5% at 1.53 mbsf. Cold-water diatoms, such as *Bacteriosira fragilis*, *Fragilariopsis cylindrus*, *Neodenticula seminae*, *Odontella aurita*, *Thalassiosira gravaida*, *Thalassiosira hyalina*, *Thalassiosira nordenskioldii*, and *Thalassiosira trifulta*, generally increase in abundance through the whole section, but sharp decreases occur at ~21.59 and 9.16 mbsf.

Td (Diatom Temperature) Value

Td value is very low and is punctuated in brief intervals by relatively larger fluctuations of 2.5%–5.0% throughout the section. The maxi-

F2. Diatom abundance vs. subbottom depth, Hole 1150A, p. 11.



mum value is 16.81% at 1.53 mbsf. These fluctuations represent changes in the surface water temperature, probably caused by the mixing of warm water and cold water in the frontal area.

Sublittoral Diatoms

Major fluctuations among secondary, smaller fluctuations in the abundance of sublittoral diatoms are recognized as declining through the whole section. The abundance of sublittoral diatoms remarkably decreases in the upper 0–5.00 mbsf. The increases in abundance of *Delphineis surirella*, *Paralia sulcata*, and *Stephanopyxis turris* occur in four intervals: 21.40–23.10, 15.80–19.60, 11.30–13.70, and 6.40–8.00 mbsf.

Freshwater Diatoms

The increased frequencies of *Aulacosira granulata*, *Eunotia* spp., and *Pinnularia* spp. are recognized in two intervals: 21.60–23.50 and 6.00–11.90 mbsf.

Extinct Diatoms

The sawtoothed curve consisting of a triple increase in abundance is recognized throughout the section. The sawtooth pattern is remarkably sharp in the upper 0–10.00 mbsf. *Melosira albicans* and *Pseudopodosira elegans* are dominant throughout the section.

Principal Component Analysis

The six highest principal components, which were chosen by plotting the eigenvalues of 33 species, are significant for the species composition because they explain 51.1% of the total variance (Fig. F3; Table T3).

The first principal component is fairly stable and shows high positive scores for the upper 3.00 mbsf. It suggests inflow of the Tsugaru Warm Current because of the mixed assemblage consisting of cold-water, warm-water, and oceanic species. On the other hand, negative scores consisting of cold-water and sublittoral species indicate a coastal area nearshore in the subarctic ocean (Table T4).

The second component shows positive scores consisting of dominant sublittoral and extinct diatoms at 19.00–23.00 and 6.00–10.00 mbsf. Negative scores consisting of exclusively cold-water and oceanic species are dominant in the upper 6.00 mbsf.

The third component is negative in the lower part of the section studied but positive in the upper part. The positive scores represent dominant cold-water and oceanic species, and the negative scores represent cold-water and sublittoral diatoms.

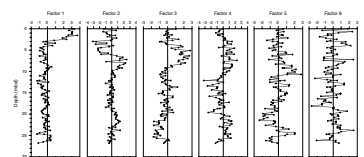
The positive scores of the fourth factor occur in the lower 20.00–26.00 mbsf and in the upper 2.00–10.00 mbsf. They are composed of extinct and cold-water species. The fifth and sixth factors are unstable and keep fluctuating throughout the section.

Hole 1151C

Diatom Abundance

Large-scale fluctuations in diatom abundance that are composed of smaller fluctuations are also recognized in the section studied from Site

F3. Q-mode principal component analysis, Hole 1150A, p. 12.



T3. Eigenvalue and percentage of variance of four significant components, Hole 1150A, p. 17.

T4. Loading for 33 species in each component, Hole 1150A, p. 18.

1151. Diatoms are generally abundant in the lower part but indicate a decline in abundance from the bottom upward throughout the section (Fig. F4). That tendency is opposite to that recognized at Site 1150. The maximum value is $10.29 \times 10^7/g$ at 18.40 and 21.40 mcd, and the minimum is $0.46 \times 10^7/g$ at 1.85 mcd. The average value, $4.4 \times 10^7/g$, is ~60% of that at northern Site 1150.

Warm-Water and Cold-Water Diatoms

Warm-water diatoms such as *Alveus marinus*, *F. doliolus*, *Roperia tessellata*, and *T. leptopus* are abundant at a maximum of 15% at 19.60 mcd in the lower part, but they are a minor component in the section. Cold-water diatoms such as *B. fragilis*, *N. seminae*, *O. aurita*, *T. gravida*, *T. hyalina*, *T. nordenskiöldii*, and *T. trifulta* increase with sharp fluctuations from the bottom to the top throughout the section.

Td (Diatom Temperature) Value

The high Td value, 35.71% at 19.60 mcd in the lower part of the section, comes from the decrease of cold-water diatoms and from the increase of warm-water diatoms. The major increases occur at 19.60, ~13.00, 7.00, and 1.85 mcd.

Sublittoral Diatoms

The abundance curve of sublittoral diatoms is marked by three sharp drops occurring at ~15.40, 7.00, and 1.00 mcd. Remarkably high abundances of *S. turris* are present at 3.70 mcd. The variation in abundance is composed of secondary, smaller fluctuations.

Freshwater Diatoms

The abundance of freshwater diatoms increases toward the top of the section, and high values of *Cyclotella* spp. and *Stephanodiscus* spp. are present at 1.85 mcd.

Extinct Diatoms

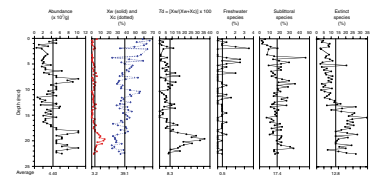
In the lower part of the section, the abundance of *M. albicans*, *P. elegans*, and *T. nidulus* increases upward and then drops at 12.80 mcd. In the upper section, the abundance gradually decreases with a peak at 5.20 mcd.

Principal Component Analysis

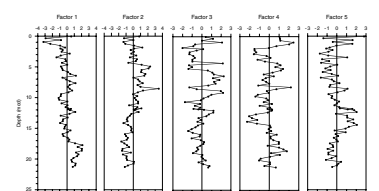
Five principal components were selected as significant based upon the eigenvalues of 34 species because they explain 46.7% of the total variance (Fig. F5; Table T5).

The first factor changes scores from high and positive in the bottom part to lower in the upper part with punctuations by several negative scores. The negative scores are remarkable in the upper 2.00 mbsf. The positive scores are composed of warm-water and oceanic diatoms, suggesting the influence of the Kuroshio Warm Current. On the other hand, the negative scores consist exclusively of cold-water and oceanic diatoms, which are dominant in this area. These fluctuations suggest an overall decline in sea-surface temperature toward the present day (Table T6).

F4. Diatom abundance vs. composite depth, Hole 1151C, p. 13.



F5. Q-mode principal component analysis, Hole 1151C, p. 14.



T5. Eigenvalue and percentage of variance of four significant components, Hole 1151C, p. 20.

T6. Loading for 34 species in each component, Hole 1151C, p. 21.

Contrary to the first, the second factor shows negative scores in the bottom part and positive scores in the upper 9.50–5.00 mbsf. Sublittoral and cold-water diatoms represent the positive scores, and extinct diatoms and warm-water diatoms represent the negative scores.

The third factor fluctuates between negative and positive scores throughout the section. The amplitudes increase upward. The positive scores are represented exclusively by cold-water and extinct diatoms, but the negative scores are attributed to sublittoral and cold-water diatoms.

The fourth factor shows the negative scores at ~14.00 mbsf and positive scores in the upper part. The interval from 19.50 to 15.00 mbsf is occupied by positive scores, which are composed of both cold-water and warm-water diatoms and oceanic diatoms. The negative scores are represented by the mixed assemblage of sublittoral, oceanic, extinct, and cold-water diatoms, and no warm-water diatoms are included.

The fifth factor fluctuates throughout the section.

DISCUSSION

There are no other useful age assignments than two diatom datums for the last occurrence of *P. curvirostris* and *T. nidulus*. The last occurrence of *P. curvirostris* is present at 51.03 mbsf in Hole 1150A and at 11.50 mcd in Hole 1151C. This datum level is almost synchronous with 0.3 Ma in middle-high latitudes in the western North Pacific Ocean (Koizumi and Tanimura, 1985; Koizumi, 1992). The assigned age is also nearly isochronous in the area along the California margin (Maruyama, 2000). The last occurrence of *T. nidulus* is recognized at 10.13 mcd in Hole 1151C. This datum level is slightly earlier in low–middle latitudes (0.39 Ma) than in middle–high latitudes (0.28 Ma) (Koizumi and Tanimura, 1985; Koizumi, 1992).

Diatom abundance seems to be greater in interglacials in Hole 1150A (Fig. F2). The high values at ~1.50 mbsf could be included within Stage 1 (Holocene), those at 17.00 mbsf within Substage 5e, and those at 26.20 mbsf within Stage 7. The sedimentation rate is possibly lower in the glacial stages, but reworked and displaced diatoms are more common when sea level lowered. *Td* values are less reliable because the value of *Xw* is smaller.

High *Td* values at 19.60 mcd in Hole 1151C correspond to the warm period at ~50 ka (Koizumi, 1994), when warm water and cold water mixed over the studied area off the Sanriku coast. Diatom abundances in Hole 1151C show a tendency to increase in interglacials as in Hole 1150A (Fig. F4). The high value at the interval from 8.52 to 7.91 mcd in Hole 1151C seems to correspond to Substage 5e based on the cyclicity of diatom abundance and sedimentation rate. The lower values of diatom abundance suggest the possibility that part of the core top might be missing.

ACKNOWLEDGMENTS

We wish to thank the Ocean Drilling Program, Texas A&M University, for furnishing the samples (sample request number 16763A) for this study. We thank the co-chief scientists, shipboard scientists, technicians, and crew of the *JOIDES Resolution* for their assistance and cooperation in obtaining the samples. Our thanks is also extended to Dr. T.

Irino, Hokkaido University, for his help and advice. Also we express our gratitude to Dr. J.A. Barron of the U.S. Geological Survey and Dr. A. Yu Gladenkov of the Geological Institute of Russian Academy of Sciences of reviewers. Gigi Delgado remarked on editorial comments.

This research used samples provided by the Ocean Drilling Program (ODP). ODP is sponsored by the U.S. National Science Foundation (NSF) and participating countries under management of Joint Oceanographic Institutions (JOI), Inc.

REFERENCES

- Kanaya, T., and Koizumi, I., 1966. Interpretation of diatom thanatocoenoses from the North Pacific applied to a study of core V20-130 (studies of a deep-sea core V20-120, part IV). *Sci. Rep. Tohoku Univ. Ser. 2*, 37:89–130.
- Kawai, H., 1972. Hydrography of the Kuroshio Extension. In Stommel, H., and Yoshida, K. (Eds.), *Kuroshio—Its Physical Aspects*: Tokyo (Univ. Tokyo Press), 235–352.
- Koizumi, I., 1985. Late Neogene paleoceanography in the western North Pacific. In Heath, G.R., Burckle, L.H., et al., *Init. Repts. DSDP*, 86: Washington (U.S. Govt. Printing Office), 429–438.
- , 1992. Diatom biostratigraphy of the Japan Sea: Leg 127. In Pisciotta, K.A., Ingle, J.C., Jr., von Breymann, M.T., Barron, J., et al., *Proc. ODP, Sci. Results*, 127/128 (Pt. 1): College Station, TX (Ocean Drilling Program), 249–289.
- , 1994. Spectral analysis of the diatom paleotemperature records at DSDP Sites 579 and 580 near the subarctic front in the western North Pacific. *Palaeogeogr., Palaeoclimatol., Palaeoecol.*, 108:475–485.
- Koizumi, I., and Tanimura, Y., 1985. Neogene diatom biostratigraphy of the middle latitude western North Pacific, Deep Sea Drilling Project Leg 86. In Heath, G.R., Burckle, L.H., et al., *Init. Repts. DSDP*, 86: Washington (U.S. Govt. Printing Office), 269–300.
- Maruyama, T., 2000. Middle Miocene to Pleistocene diatom stratigraphy of Leg 167. In Lyle, M., Koizumi, I., Richter, C., and Moore, T.C., Jr. (Eds.), *Proc. ODP, Sci. Results*, 167: College Station, TX (Ocean Drilling Program), 63–110.
- Sacks, I.S., Suyehiro, K., Acton, G.D., et al., 2000. *Proc. ODP, Init. Repts.*, 186 [CD-ROM]. Available from: Ocean Drilling Program, Texas A&M University, College Station TX 77845-9547, USA.
- Takemoto, A., and Oda, M., 1997. New planktic foraminiferal transfer functions for the Kuroshio-Oyashio Current region off Japan. *Paleontol. Res.*, 1:291–310.

Figure F1. Location of ODP Leg 186 Sites 1150 and 1151. Major current systems and the generalized distribution of sea-surface water masses in seas adjacent to the Japanese Islands are adopted from Takemoto and Oda (1997). C = areas dominated by cold-water masses during the meandering of the Kuroshio Current; W = areas dominated by warm-water masses within the so-called Perturbed Area between the Kuroshio and Oyashio Currents.

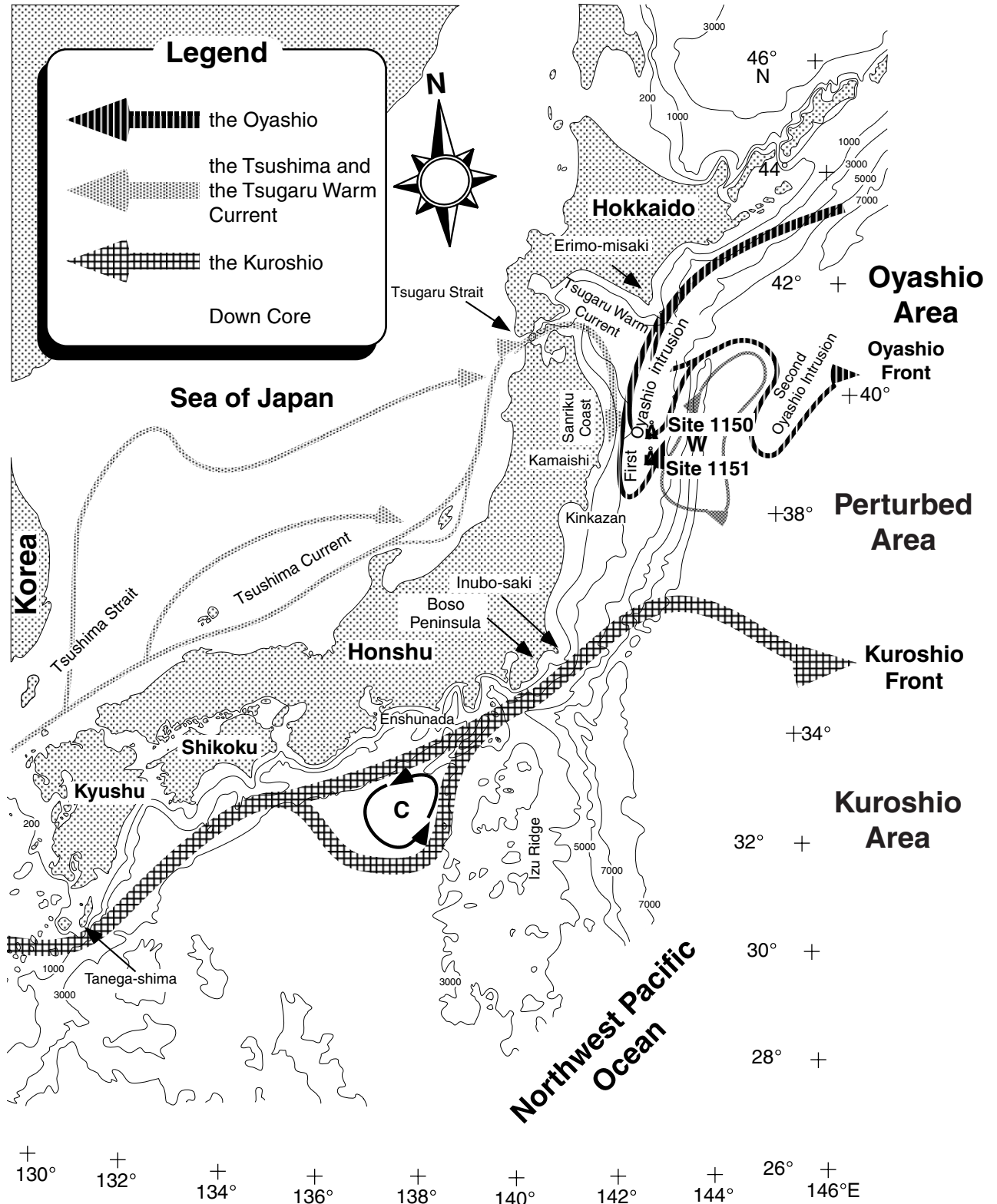


Figure F2. Stratigraphic variations of the abundance of diatoms and other paleoceanographic parameters based upon species compositions plotted against the subbottom depth (mbsf), Hole 1150A. Xw = frequency of warm-water species, Xc = frequency of cold-water species, Td = diatom temperature.

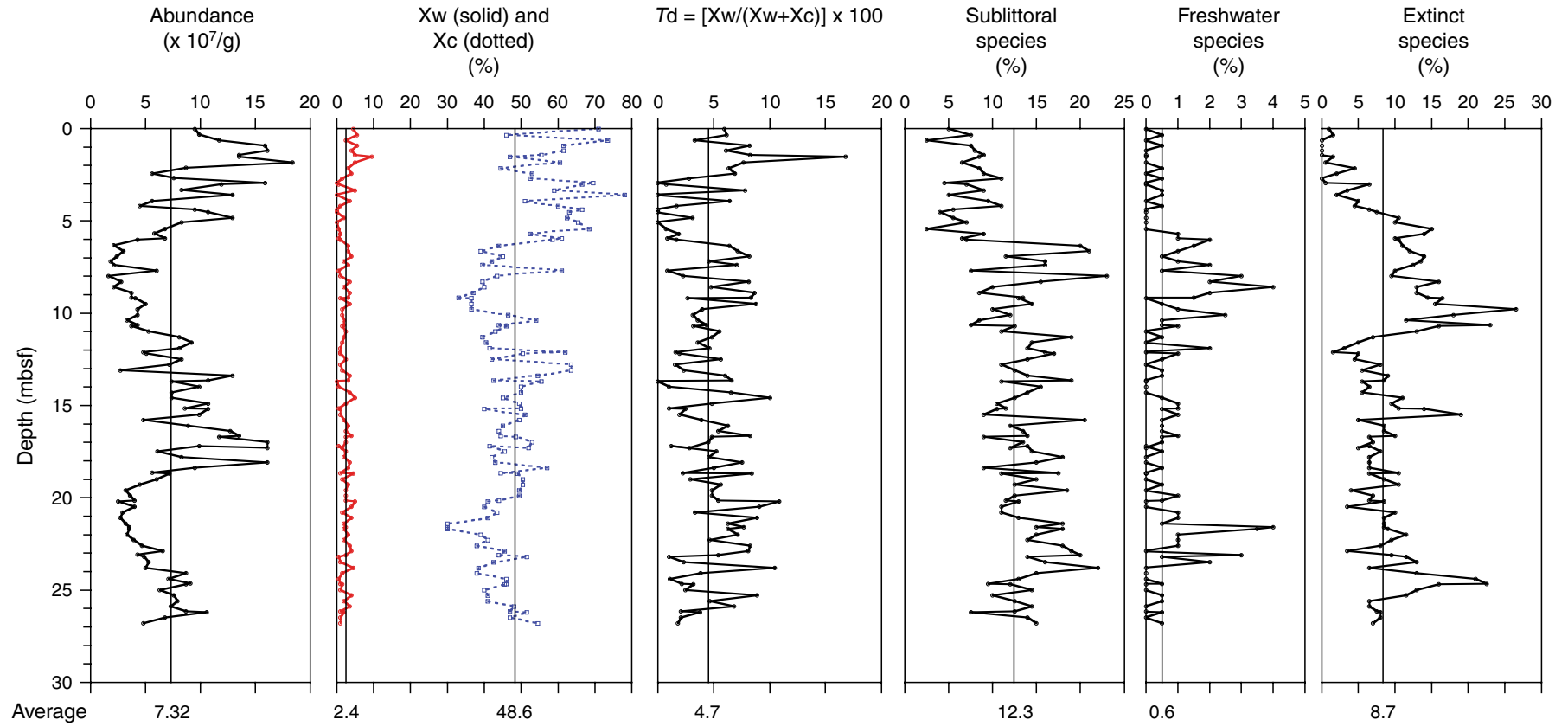


Figure F3. Stratigraphic loadings for each component of Q-mode principal component analysis of the diatom assemblage which occurs over six diatoms in any sample, Hole 1150A.

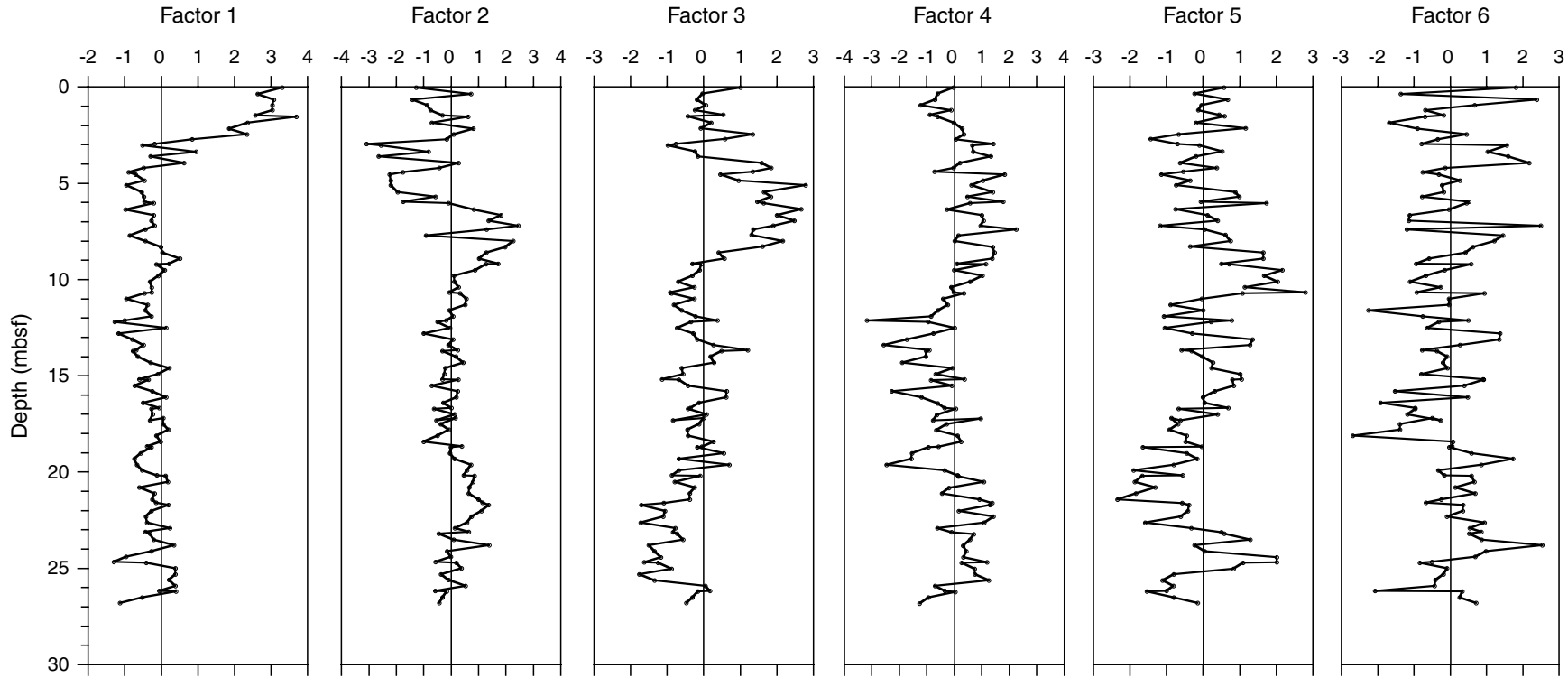


Figure F4. Stratigraphic variations of the abundance of diatoms and other paleoceanographic parameters based upon species compositions plotted against the composite depth (mcd), Hole 1151C. Xw = frequency of warm-water species, Xc = frequency of cold-water species, Td = diatom temperature.

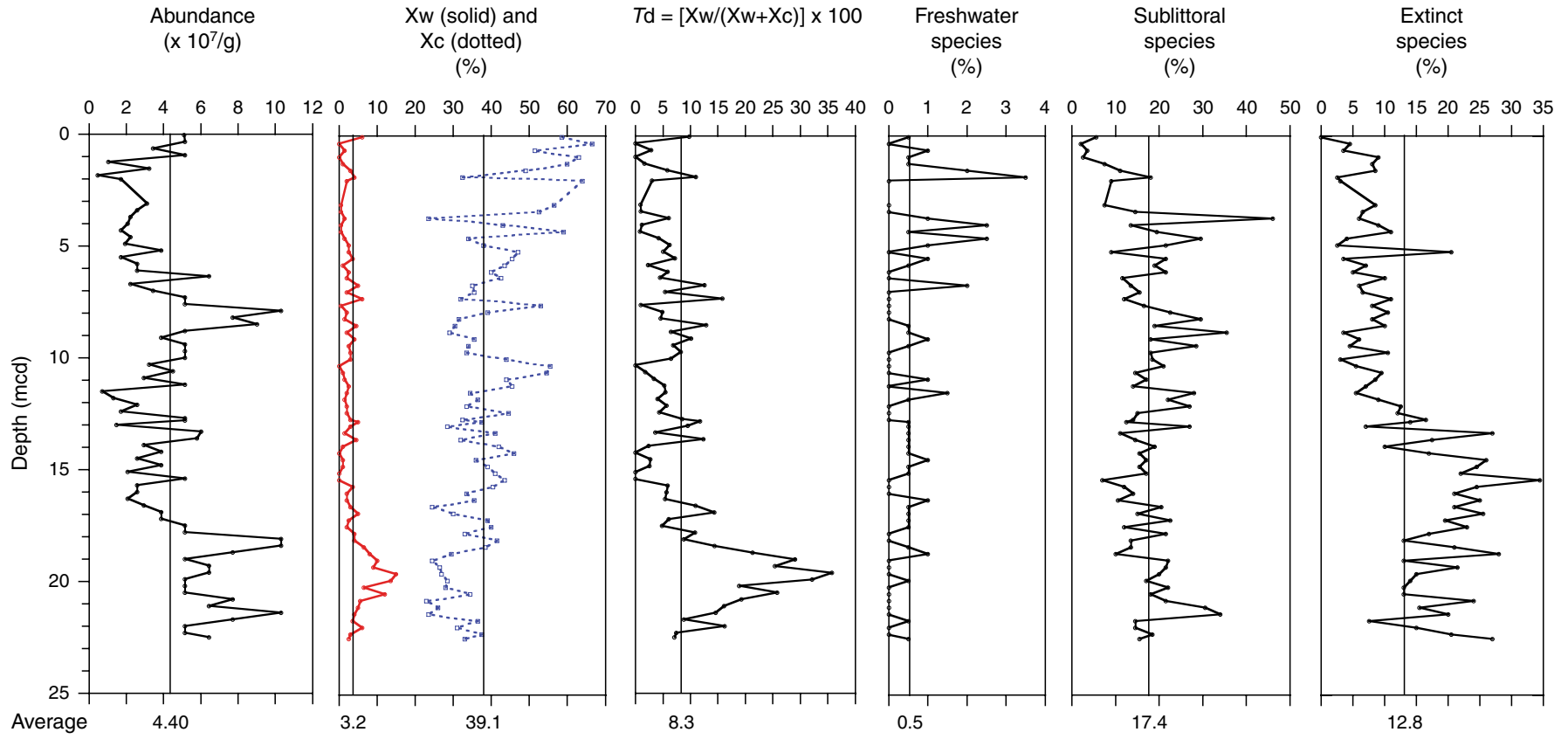


Figure F5. Stratigraphic loadings for each component of Q-mode principal component analysis of the diatom assemblage which occurs over six diatoms in any sample, Hole 1151C. The subbottom depth (mbsf) is used.

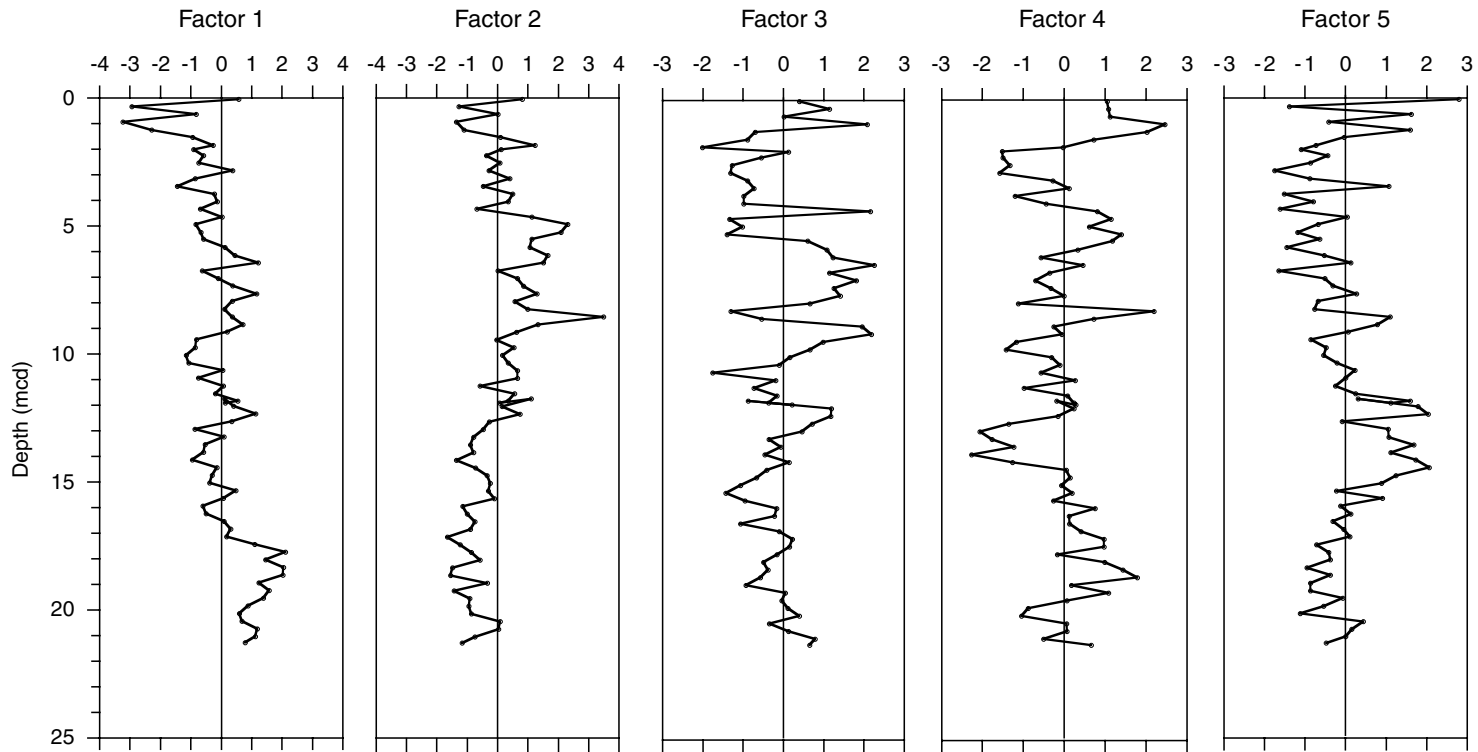


Table T1. Distribution chart of diatom species, Hole 1150A. (This table is available in an [oversized format](#).)

Table T2. Distribution chart of diatom species, Hole 1151C. (This table is available in an [oversized format](#).)

Table T3. Eigenvalue and percentage of variance of four significant components, Hole 1150A.

Component	Eigenvalue	Percent of variance explained	Cumulative percent of variance explained
1	4.952	15.0	15.0
2	4.439	13.5	28.5
3	2.555	7.7	36.2
4	1.957	5.9	42.1
5	1.728	5.2	47.4
6	1.376	4.2	51.5

Table T4. Loading for 33 species in each component, Hole 1150A. (Continued on next page.)

Factor 1		Factor 2		Factor 3	
Loading	Species	Loading	Species	Loading	Species
0.8553	<i>Odontella aurita</i>	0.6360	<i>Thalassionema nitzschioides</i>	0.7938	<i>Thalassiosira trifulta</i>
0.7319	<i>Neodenticula seminae</i>	0.6114	<i>Delphineis</i> spp.	0.5311	<i>Thalassiosira antiqua</i>
0.6669	<i>Fragilariopsis doliolus</i>	0.5281	<i>Pseudopodosira elegans</i>	0.4040	<i>Thalassiosira pacifica</i>
0.5835	<i>Thalassiosira leptopus</i>	0.4767	<i>Neodenticula</i> spp.	0.3961	<i>Porosira glacialis</i>
0.4916	<i>Thalassiosira nordenskioldii</i>	0.4755	<i>Cocconeis</i> spp.	0.3327	<i>Neodenticula</i> spp.
0.4824	<i>Chaetoceros furcellatus</i>	0.4333	<i>Thalassiosira oestrupii</i>	0.3320	<i>Actinocyclus ochotensis</i>
0.4791	<i>Thalassiosira lineata</i>	0.4173	<i>Rhizosolenia styliformis</i>	0.2798	<i>Coscinodiscus oculus-iridis</i>
0.3832	<i>Rhizosolenia setigera</i>	0.4059	<i>Actinocyclus curvatulus</i>	0.2552	<i>Actinocyclus curvatulus</i>
0.3055	<i>Thalassiosira oestrupii</i>	0.3721	<i>Paralia sulcata</i>	0.2278	<i>Thalassiosira</i> cfr. <i>convexa</i>
0.2726	<i>Thalassionema nitzschioides</i>	0.3657	<i>Stephanopyxis turris</i>	0.2251	<i>Rhizosolenia styliformis</i>
0.2403	<i>Stellarima stellaris</i>	0.2973	<i>Rhizosolenia setigera</i>	0.2211	<i>Cocconeis</i> spp.
0.1825	<i>Thalassiosira pacifica</i>	0.2780	<i>Stellarima stellaris</i>	0.1852	<i>Neodenticula seminae</i>
0.1658	<i>Paralia sulcata</i>	0.2641	<i>Thalassiosira lineata</i>	0.1746	<i>Pseudopodosira elegans</i>
0.1538	<i>Rhizosolenia styliformis</i>	0.2482	<i>Thalassiosira eccentrica</i>	0.1523	<i>Chaetoceros furcellatus</i>
0.0984	<i>Porosira glacialis</i>	0.1640	<i>Fragilariopsis doliolus</i>	0.1056	<i>Stellarima stellaris</i>
0.0227	<i>Thalassiosira eccentrica</i>	0.1356	<i>Thalassiosira</i> cf. <i>convexa</i>	0.0706	<i>Fragilariopsis doliolus</i>
-0.0532	<i>Thalassiosira trifulta</i>	0.1177	<i>Coscinodiscus oculus-iridis</i>	0.0484	<i>Thalassiosira hyalina</i>
-0.1156	<i>Coscinodiscus oculus-iridis</i>	0.1088	<i>Thalassiosira leptopus</i>	0.0448	<i>Thalassiosira oestrupii</i>
-0.1515	<i>Neodenticula</i> spp.	0.0600	<i>Actinocyclus ochotensis</i>	0.0035	<i>Thalassiosira leptopus</i>
-0.1863	<i>Actinocyclus ochotensis</i>	0.0375	<i>Melosira albicans</i>	-0.00928	<i>Odontella aurita</i>
-0.2422	<i>Actinocyclus curvatulus</i>	0.0364	<i>Thalassiosira trifulta</i>	-0.03955	<i>Stephanopyxis turris</i>
-0.2444	<i>Delphineis</i> spp.	-0.03628	<i>Thalassiosira gravida</i>	-0.04342	<i>Rhizosolenia setigera</i>
-0.2502	<i>Pseudopodosira elegans</i>	-0.04335	<i>Odontella aurita</i>	-0.07551	<i>Thalassiosira gravida</i>
-0.2602	<i>Thalassiosira</i> cf. <i>convexa</i>	-0.0902	<i>Bacteriosira fragilis</i>	-0.18088	<i>Thalassiosira nordenskioldii</i>
-0.3004	<i>Thalassiosira hyalina</i>	-0.1488	<i>Thalassiosira antiqua</i>	-0.18285	<i>Fragilariopsis cylindrus</i>
-0.3235	<i>Thalassiosira antiqua</i>	-0.1837	<i>Neodenticula seminae</i>	-0.18677	<i>Delphineis</i> spp.
-0.3377	<i>Melosira albicans</i>	-0.22703	<i>Porosira glacialis</i>	-0.21292	<i>Thalassiosira lineata</i>
-0.3470	<i>Fragilariopsis cylindrus</i>	-0.36131	<i>Fragilariopsis oceanica</i>	-0.24456	<i>Fragilariopsis oceanica</i>
-0.3472	<i>Fragilariopsis oceanica</i>	-0.40022	<i>Thalassiosira pacifica</i>	-0.25138	<i>Paralia sulcata</i>
-0.3828	<i>Cocconeis</i> spp.	-0.45045	<i>Thalassiosira nordenskioldii</i>	-0.29462	<i>Thalassionema nitzschioides</i>
-0.4324	<i>Stephanopyxis turris</i>	-0.48231	<i>Chaetoceros furcellatus</i>	-0.32141	<i>Bacteriosira fragilis</i>
-0.4726	<i>Bacteriosira fragilis</i>	-0.63775	<i>Fragilariopsis cylindrus</i>	-0.32667	<i>Thalassiosira eccentrica</i>
-0.5476	<i>Thalassiosira gravida</i>	-0.70955	<i>Thalassiosira hyalina</i>	-0.35133	<i>Melosira albicans</i>

Table T4 (continued).

Factor 4		Factor 5		Factor 6	
Loading	Species	Loading	Species	Loading	Species
0.3944	<i>Pseudopodosira elegans</i>	0.5398	<i>Bacteriosira fragilis</i>	0.3783	<i>Actinocyclus ochotensis</i>
0.3059	<i>Thalassiosira hyalina</i>	0.5265	<i>Melosira albicans</i>	0.3243	<i>Rhizosolenia setigera</i>
0.3012	<i>Thalassiosira cf. convexa</i>	0.4684	<i>Rhizosolenia styliformis</i>	0.3241	<i>Chaetoceros furcellatus</i>
0.2581	<i>Porosira glacialis</i>	0.2868	<i>Thalassiosira cf. convexa</i>	0.2838	<i>Actinocyclus curvatulus</i>
0.2544	<i>Fragilariopsis cylindrus</i>	0.2019	<i>Coscinodiscus oculus-iridis</i>	0.2774	<i>Paralia sulcata</i>
0.2368	<i>Actinocyclus curvatulus</i>	0.1998	<i>Porosira glacialis</i>	0.1861	<i>Thalassiosira gravida</i>
0.2156	<i>Melosira albicans</i>	0.1904	<i>Thalassiosira lineata</i>	0.1678	<i>Fragilariopsis cylindrus</i>
0.2148	<i>Thalassiosira eccentrica</i>	0.1265	<i>Odontella aurita</i>	0.1676	<i>Stellarima stellaris</i>
0.2005	<i>Delphineis</i> spp.	0.1259	<i>Fragilariopsis doliolus</i>	0.1273	<i>Neodenticula seminae</i>
0.1902	<i>Rhizosolenia styliformis</i>	0.0778	<i>Actinocyclus ochotensis</i>	0.1176	<i>Thalassiosira hyalina</i>
0.1766	<i>Neodenticula</i> spp.	0.0474	<i>Rhizosolenia setigera</i>	0.1121	<i>Thalassiosira lineata</i>
0.1700	<i>Stellarima stellaris</i>	0.0119	<i>Pseudopodosira elegans</i>	0.0976	<i>Cocconeis</i> spp.
0.1678	<i>Rhizosolenia setigera</i>	-0.0026	<i>Chaetoceros furcellatus</i>	0.0855	<i>Odontella aurita</i>
0.1657	<i>Thalassiosira trifulta</i>	-0.00301	<i>Thalassiosira gravida</i>	0.0827	<i>Neodenticula</i> spp.
0.1500	<i>Chaetoceros furcellatus</i>	-0.01347	<i>Thalassiosira trifulta</i>	0.0512	<i>Delphineis</i> spp.
0.0961	<i>Thalassionema nitzschioides</i>	-0.02075	<i>Neodenticula</i> spp.	0.0076	<i>Thalassiosira trifulta</i>
0.0956	<i>Fragilariopsis oceanica</i>	-0.02716	<i>Neodenticula seminae</i>	-0.00112	<i>Melosira albicans</i>
0.0611	<i>Thalassiosira lineata</i>	-0.02847	<i>Thalassiosira antiqua</i>	-0.00842	<i>Pseudopodosira elegans</i>
0.0414	<i>Thalassiosira nordenskioldii</i>	-0.03463	<i>Thalassiosira nordenskioldii</i>	-0.01956	<i>Thalassiosira leptopus</i>
0.0393	<i>Paralia sulcata</i>	-0.04001	<i>Paralia sulcata</i>	-0.0466	<i>Rhizosolenia styliformis</i>
-0.00282	<i>Thalassiosira pacifica</i>	-0.05046	<i>Thalassiosira hyalina</i>	-0.05313	<i>Thalassiosira cf. convexa</i>
-0.10214	<i>Fragilariopsis doliolus</i>	-0.07254	<i>Delphineis</i> spp.	-0.08698	<i>Bacteriosira fragilis</i>
-0.10519	<i>Thalassiosira antiqua</i>	-0.07504	<i>Thalassiosira leptopus</i>	-0.0964	<i>Fragilariopsis doliolus</i>
-0.10922	<i>Bacteriosira fragilis</i>	-0.08902	<i>Cocconeis</i> spp.	-0.10152	<i>Thalassiosira antiqua</i>
-0.11332	<i>Odontella aurita</i>	-0.12837	<i>Stephanopyxis turris</i>	-0.1372	<i>Stephanopyxis turris</i>
-0.12807	<i>Cocconeis</i> spp.	-0.1706	<i>Thalassiosira pacifica</i>	-0.17269	<i>Thalassiosira nordenskioldii</i>
-0.15369	<i>Neodenticula seminae</i>	-0.20046	<i>Fragilariopsis cylindrus</i>	-0.1728	<i>Thalassionema nitzschioides</i>
-0.20966	<i>Coscinodiscus oculus-iridis</i>	-0.20356	<i>Thalassionema nitzschioides</i>	-0.20915	<i>Thalassiosira eccentrica</i>
-0.22304	<i>Thalassiosira oestrupii</i>	-0.21003	<i>Stellarima stellaris</i>	-0.21496	<i>Fragilariopsis oceanica</i>
-0.25398	<i>Thalassiosira leptopus</i>	-0.2496	<i>Thalassiosira oestrupii</i>	-0.22168	<i>Thalassiosira pacifica</i>
-0.40523	<i>Stephanopyxis turris</i>	-0.26059	<i>Thalassiosira eccentrica</i>	-0.27603	<i>Coscinodiscus oculus-iridis</i>
-0.53882	<i>Actinocyclus ochotensis</i>	-0.41226	<i>Actinocyclus curvatulus</i>	-0.37899	<i>Porosira glacialis</i>
-0.63106	<i>Thalassiosira gravida</i>	-0.45025	<i>Fragilariopsis oceanica</i>	-0.48506	<i>Thalassiosira oestrupii</i>

Table T5. Eigenvalue and percent of variance of four significant components, Hole 1151C.

Components	Eigenvalue	Percent of variance explained	Cumulative percent of variance explained
1	5.41976	15.9	15.9
2	3.85656	11.3	27.3
3	2.56484	7.5	34.8
4	2.21086	6.5	41.3
5	1.79674	5.3	46.6

Table T6. Loading for 34 species in each component, Hole 1151C.

Factor 1		Factor 2		Factor 3		Factor 4		Factor 5	
Loading	Species	Loading	Species	Loading	Species	Loading	Species	Loading	Species
0.6549	<i>Thalassiosira leptopus</i>	0.7117	<i>Delphineis</i> spp.	0.6230	<i>Thalassiosira nordenskiöldii</i>	0.5253	<i>Actinocyclus curvatus</i>	0.5699	<i>Thalassiosira trifulta</i>
0.6172	<i>Fragilariopsis doliolus</i>	0.6539	<i>Thalassionema nitzschioides</i>	0.5180	<i>Rhizosolenia styliformis</i>	0.4661	<i>Thalassiosira decipiens</i>	0.5606	<i>Neodenticula seminae</i>
0.5775	<i>Thalassiosira oestrupii</i>	0.6241	<i>Cyclotella striata</i>	0.5018	<i>Thalassiosira antiqua</i>	0.4355	<i>Thalassiosira hyalina</i>	0.4676	<i>Thalassiosira nidulus</i>
0.5562	<i>Thalassiosira eccentrica</i>	0.6214	<i>Paralia sulcata</i>	0.4587	<i>Thalassiosira hyalina</i>	0.4210	<i>Thalassiosira leptopus</i>	0.4348	<i>Odontella aurita</i>
0.5380	<i>Roperia tessellata</i>	0.4459	<i>Rhizosolenia hebetata</i>	0.3464	<i>Melosira albicans</i>	0.3580	<i>Actinocyclus ochotensis</i>	0.2799	<i>Pseudopodosira elegans</i>
0.4721	<i>Thalassiosira pacifica</i>	0.4017	<i>Coscinodiscus marginatus</i>	0.3162	<i>Neodenticula seminae</i>	0.3077	<i>Fragilariopsis doliolus</i>	0.1780	<i>Paralia sulcata</i>
0.3953	<i>Stephanopyxis turris</i>	0.4007	<i>Rhizosolenia styliformis</i>	0.3069	<i>Porosira glacialis</i>	0.3017	<i>Thalassiosira pacifica</i>	0.1679	<i>Chaetoceros furcellatus</i>
0.3697	<i>Melosira albicans</i>	0.3794	<i>Thalassiosira antiqua</i>	0.1700	<i>Bacteria fragilis</i>	0.2827	<i>Roperia tessellata</i>	0.1225	<i>Thalassiosira oestrupii</i>
0.3491	<i>Thalassiosira cf. convexa</i>	0.2526	<i>Neodenticula seminae</i>	0.1485	<i>Fragilariopsis cylindrus</i>	0.2664	<i>Cyclotella striata</i>	0.1155	<i>Rhizosolenia styliformis</i>
0.3159	<i>Rhizosolenia styliformis</i>	0.2231	<i>Porosira glacialis</i>	0.1293	<i>Chaetoceros furcellatus</i>	0.2577	<i>Coscinodiscus marginatus</i>	0.1099	<i>Thalassiosira decipiens</i>
0.2227	<i>Thalassiosira antiqua</i>	0.1345	<i>Thalassiosira nordenskiöldii</i>	0.0967	<i>Paralia sulcata</i>	0.2351	<i>Thalassiosira cf. convexa</i>	0.0940	<i>Porosira glacialis</i>
0.2200	<i>Neodenticula seminae</i>	0.1140	<i>Cocconeis</i> spp.	0.0937	<i>Fragilariopsis oceanica</i>	0.2158	<i>Odontella aurita</i>	0.0637	<i>Coscinodiscus marginatus</i>
0.1653	<i>Paralia sulcata</i>	0.0950	<i>Odontella aurita</i>	0.0859	<i>Thalassiosira decipiens</i>	0.2088	<i>Fragilariopsis cylindrus</i>	0.0341	<i>Thalassiosira leptopus</i>
0.1161	<i>Thalassionema nitzschioides</i>	0.0875	<i>Actinocyclus curvatus</i>	0.0397	<i>Thalassiosira leptopus</i>	0.2047	<i>Bacteria fragilis</i>	0.0248	<i>Thalassiosira antiqua</i>
0.0780	<i>Actinocyclus ochotensis</i>	0.0472	<i>Thalassiosira eccentrica</i>	0.0305	<i>Thalassiosira eccentrica</i>	0.1795	<i>Neodenticula seminae</i>	0.0242	<i>Thalassiosira pacifica</i>
0.0645	<i>Thalassiosira nidulus</i>	0.0194	<i>Bacteria fragilis</i>	0.0120	<i>Rhizosolenia hebetata</i>	0.1777	<i>Thalassiosira nordenskiöldii</i>	-0.00955	<i>Rhizosolenia hebetata</i>
0.0343	<i>Cyclotella striata</i>	-0.08138	<i>Thalassiosira oestrupii</i>	-0.00794	<i>Thalassiosira oestrupii</i>	0.1706	<i>Melosira albicans</i>	-0.01192	<i>Cyclotella striata</i>
-0.01106	<i>Coscinodiscus marginatus</i>	-0.08335	<i>Thalassiosira hyalina</i>	-0.02482	<i>Odontella aurita</i>	0.1442	<i>Delphineis</i> spp.	-0.02005	<i>Thalassiosira cf. convexa</i>
-0.02371	<i>Odontella aurita</i>	-0.09457	<i>Thalassiosira leptopus</i>	-0.06348	<i>Thalassiosira pacifica</i>	0.1302	<i>Thalassionema nitzschioides</i>	-0.02989	<i>Fragilariopsis oceanica</i>
-0.05028	<i>Rhizosolenia hebetata</i>	-0.12825	<i>Fragilariopsis cylindrus</i>	-0.06409	<i>Roperia tessellata</i>	0.1247	<i>Thalassiosira trifulta</i>	-0.03011	<i>Actinocyclus ochotensis</i>
-0.12254	<i>Porosira glacialis</i>	-0.15343	<i>Thalassiosira gravida</i>	-0.09966	<i>Stephanopyxis turris</i>	0.0811	<i>Thalassiosira eccentrica</i>	-0.04104	<i>Actinocyclus curvatus</i>
-0.18209	<i>Thalassiosira nordenskiöldii</i>	-0.15545	<i>Stephanopyxis turris</i>	-0.10366	<i>Thalassiosira trifulta</i>	0.0593	<i>Paralia sulcata</i>	-0.05338	<i>Thalassiosira eccentrica</i>
-0.22148	<i>Cocconeis</i> spp.	-0.19212	<i>Actinocyclus ochotensis</i>	-0.10814	<i>Fragilariopsis doliolus</i>	0.0521	<i>Fragilariopsis oceanica</i>	-0.05815	<i>Cocconeis</i> spp.
-0.22717	<i>Delphineis</i> spp.	-0.204	<i>Thalassiosira trifulta</i>	-0.10877	<i>Thalassiosira gravida</i>	0.0010	<i>Pseudopodosira elegans</i>	-0.06677	<i>Melosira albicans</i>
-0.24008	<i>Actinocyclus curvatus</i>	-0.20748	<i>Fragilariopsis oceanica</i>	-0.12371	<i>Thalassiosira cf. convexa</i>	-0.03718	<i>Porosira glacialis</i>	-0.07005	<i>Delphineis</i> spp.
-0.29504	<i>Chaetoceros furcellatus</i>	-0.25431	<i>Thalassiosira pacifica</i>	-0.17789	<i>Pseudopodosira elegans</i>	-0.04625	<i>Cocconeis</i> spp.	-0.11585	<i>Fragilariopsis doliolus</i>
-0.36253	<i>Thalassiosira trifulta</i>	-0.27003	<i>Melosira albicans</i>	-0.20315	<i>Thalassiosira nidulus</i>	-0.04962	<i>Chaetoceros furcellatus</i>	-0.14676	<i>Thalassiosira nordenskiöldii</i>
-0.37148	<i>Bacteria fragilis</i>	-0.27109	<i>Pseudopodosira elegans</i>	-0.24724	<i>Actinocyclus curvatus</i>	-0.07334	<i>Rhizosolenia hebetata</i>	-0.16243	<i>Thalassionema nitzschioides</i>
-0.4899	<i>Thalassiosira hyalina</i>	-0.27284	<i>Chaetoceros furcellatus</i>	-0.27569	<i>Cyclotella striata</i>	-0.07569	<i>Thalassiosira antiqua</i>	-0.16919	<i>Thalassiosira hyalina</i>
-0.52371	<i>Thalassiosira gravida</i>	-0.2886	<i>Thalassiosira decipiens</i>	-0.30884	<i>Actinocyclus ochotensis</i>	-0.10616	<i>Rhizosolenia styliformis</i>	-0.20282	<i>Roperia tessellata</i>
-0.55322	<i>Thalassiosira decipiens</i>	-0.32495	<i>Fragilariopsis doliolus</i>	-0.31703	<i>Thalassionema nitzschioides</i>	-0.16153	<i>Thalassiosira oestrupii</i>	-0.20474	<i>Thalassiosira gravida</i>
-0.60415	<i>Pseudopodosira elegans</i>	-0.43623	<i>Roperia tessellata</i>	-0.3287	<i>Delphineis</i> spp.	-0.30536	<i>Thalassiosira nidulus</i>	-0.28645	<i>Fragilariopsis cylindrus</i>
-0.60432	<i>Fragilariopsis cylindrus</i>	-0.44145	<i>Thalassiosira nidulus</i>	-0.39615	<i>Coscinodiscus marginatus</i>	-0.39006	<i>Thalassiosira gravida</i>	-0.37253	<i>Bacteria fragilis</i>
-0.82055	<i>Fragilariopsis oceanica</i>	-0.50032	<i>Thalassiosira cf. convexa</i>	-0.54499	<i>Cocconeis</i> spp.	-0.41633	<i>Stephanopyxis turris</i>	-0.37756	<i>Stephanopyxis turris</i>